UMTRI-2016-15

Development of Geometric Specifications for a Small Female Anthropomorphic Test Device Pelvis

Katelyn F. Klein
Matthew P. Reed
Jonathan D. Rupp

April 2016

UMTRI-2016-15

Development of Geometric Specifications for a Small Female Anthropomorphic Test Device Pelvis

Katelyn F. Klein
Matthew P. Reed
Jonathan D. Rupp

The University of Michigan
Transportation Research Institute
Ann Arbor, MI 48109-2150
U.S.A.

April 2016

Technical Report Documentation Page

1. Report No.	2. Government Accession No.	3. Recipient's Catalog No.
UMTRI-2016-15		

4. Title and Subtitle Development of Geometric Specifications for a Small Female Anthropomorphic Test Device Pelvis	5. Report Date April 2016 6. Performing Organization Code 063908
7. Author(s) Klein, K. F., Reed, M. P., and Rupp, J. D.	8. Performing Organization Report No. UMTRI-2016-15
9. Performing Organization Name and Address The University of Michigan Transportation Research Institute 2901 Baxter Road Ann Arbor, Michigan 48109-2150 U.S.A.	10. Work Unit no. (TRAIS) 11. Contract or Grant No.
12. Sponsoring Agency Name and Address U.S. Department of Transportation National Highway Traffic Safety Administration 1200 New Jersey Avenue, SE Washington, DC 20590	13. Type of Report and Period Covered 14. Sponsoring Agency Code

15. Supplementary Notes

16. Abstract

Target surface geometry for the small female anthropomorphic test device pelvis was predicted by a statistical pelvis geometry model developed through analysis of medical imaging data. The resulting geometry was compared to the Hybrid III small female pelvis geometry and an estimate of female pelvis geometry obtained by length scaling the midsize male pelvis based on bispinous breadth. Differences were found in the shape of the pubic rami, ischial tuberosities, and anterior superior iliac wings between the small female pelvis model and the Hybrid III pelvis, which may affect interactions with seat belts and vehicle structures.

17. Key Words	18. Distribution Statement
Occupant characteristics, Motor vehicle crashes, Statistical models	Unlimited

19. Security Classification (of this report)	20. Security Classification (of this page)	21. No. of Pages	22. Price
None	None	16	

Contents

Contents iii
List of Figures iii
List of Tables iii
1 Introduction 3
2 Methods 4
  2.1 Statistical Model Development 4
  2.2 Comparison of Pelvis Models 4
3 Results 5
  3.1 Female Pelvis Model Geometry 5
  3.2 Comparison of Pelvis Models 6
4 Discussion and Conclusions 9
Appendix A – Small Female Pelvis Landmark Coordinates 100
Acknowledgements 122
References 133

List of Figures

Figure 1a. Small female pelvis geometry predicted by a statistical pelvis geometry model. 5
Figure 1b. Small female pelvis geometry made symmetric by reflecting the left side to the right. 5
Figure 2. Comparison of SFPM geometry and Hybrid III geometry. 7
Figure 3a. Comparison of SFPM geometry and Hybrid III geometry aligned to ischial tuberosities. 7
Figure 3b. Comparison of SFPM geometry and Hybrid III geometry aligned to hip joint centers. 8
Figure 4. Comparison of SFPM geometry and scaled male geometry. 8

List of Tables

Table 1. Comparison of small female pelvis model, AMVO, small female Hybrid III, and scaled midsize male model dimensions. 6

1 Introduction

Multiple studies have demonstrated sex-related differences in types and risk of lower extremity injuries in motor vehicle crashes (e.g., Carter et al. 2014; Rupp and Flannagan 2011). These differences are thought to be in part due to sex-related differences in the sizes and shapes of lower extremity bones that affect the interaction between the body and the vehicle seat and restraint system (Besnault et al. 1998; Riggs et al. 2004; Wang et al. 2004). As a result, for crash test dummies or anthropomorphic test devices (ATDs) to reproduce sex-specific differences in lower extremity injury type and risk, they must appropriately capture the sex-specific differences in skeletal and soft tissue geometry. In the pelvis, it is critical for the size and shape of the iliac wings to be humanlike to have realistic interaction with seat belts and vehicle structures. The ischial tuberosities also must be in the correct location for reasonable interaction with vehicle seats.

Despite differences between the sexes in lower extremity bone shape, the shapes of female ATD skeletal components have typically been established by scaling male geometry, usually based on a characteristic length (Schneider et al. 1983; Rhule and Backaitis 1998; Humanetics Innovative Solutions, Plymouth, MI). As a result, the bones of small female ATDs may have the appropriate size (or an appropriate correct dimension), but not a representative shape. In the pelvis, sex-specific differences in shape exist that may affect the interaction of the pelvis with vehicle belts and side structures (Wang et al. 2004). One way to account for this would be to use a single female pelvis as the ATD design target; however, such an approach does not necessarily result in a pelvis that has the typical size and shape. A better approach is to use a pelvis described by averaging skeletal surface landmark locations for a particular range of sizes, as was done by Reynolds et al. (1981). In this study, landmark locations were averaged from all pelvises from women under the 25th percentile in height in a sample of post-mortem pelvises; however, this approach involves some averaging and is somewhat limited by the idiosyncrasies of the sample.

A still better approach is to use a statistical shape model that is based on a large number of pelvises to predict the geometry associated with a particular set of occupant characteristics. An early attempt to develop such a parametric model of the pelvis by Besnault et al. (1998) did not consider occupant characteristics, such as age and BMI, which affect injury risk. The first known definition of an ATD skeletal component via statistical shape analysis was the pediatric pelvis developed by Reed et al. (2009) and tested by Klinich et al. (2010). Later work by Klein (2015) resulted in statistical geometry models for the male and female pelvises that are parameterized by age, BMI, and bispinous breadth. In this report, the surface geometry for the small female pelvis is predicted using the Klein (2015) female pelvis model. The resulting geometry is compared to the Hybrid III small female pelvis geometry and an estimate of female pelvis geometry obtained by length scaling the midsize male pelvis based on bispinous breadth.

2 Methods

2.1 Statistical Model Development

The steps for developing statistical models of pelvis geometry are described in detail in Klein (2015). Bone geometry was extracted from 58 male and 77 female clinical CT scans and a template FE mesh was fit to the surface geometries. Principal component analysis was then performed on the nodal coordinates, and linear regression models were developed to predict the principal component scores to predict geometry as functions of age, BMI, and bispinous breadth for men and women. A complete pelvis can then be reconstructed from the principal component scores.

Target geometry for the small female pelvis was predicted using a statistical model developed from only female data with inputs of age equal to 40 years, BMI equal to 22 kg/m^2, and bispinous breadth equal to 206 mm. The latter two parameters correspond to the Anthropometry of Motor Vehicle Occupants (AMVO) specification for the small female (Schneider et al. 1983). An age of 40 years was developed prior to the current study as the desired target. This age approximates the mean age of 37 years of a female adult occupant involved in a tow-away crash in the United States based on data from the National Automotive Sampling System-Crashworthiness Data System 2001-2013. The model generated using this method is referred to as the small female pelvis model (SFPM) in the subsequent text. Since the SFPM is not symmetric, the model was made symmetric for comparison to the AMVO and Hybrid III geometry by reflecting the left side about the midline to generate the right side.

2.2 Comparison of Pelvis Models

The symmetric SFPM was compared to small female pelvis dimensions from the AMVO reports, the small female (5th percentile) Hybrid III ATD pelvis (Humanetics Innovative Solutions, Plymouth, MI), and geometry obtained by applying uniform length scaling techniques to an average midsize male pelvis. Length scaling was based on the AMVO target for bispinous breadth (small female target bispinous breadth = 206 mm; midsize male bispinous breadth = 242 mm). The midsize male pelvis geometry was generated using a statistical male pelvis model (Klein 2015) with the inputs of age equal to 40 years, BMI equal to 25 kg/m^2, and bispinous breadth equal to 242 mm. This model has a homologous mesh with the same number of nodes as the statistical model of the small female pelvis, and thus, positions of corresponding nodes representing skeletal surface landmarks can be compared.

3 Results

3.1 Female Pelvis Model Geometry

The SFPM is shown in Figure 1a, and the symmetric SFPM is shown in Figure 1b. All right landmarks on the SFPM are within 4 mm (most are within 2 mm) of the reflected contralateral landmarks used to develop the symmetric SFPM. The landmark coordinates are listed in Appendix A, and the nodal coordinates for the symmetric SFPM are available electronically (doi:10.7302/Z2BZ63ZM). Note that the left-to-right reflection process reduced the target bispinous breadth (206 mm) to the new bispinous breadth for the symmetric model (204 mm).

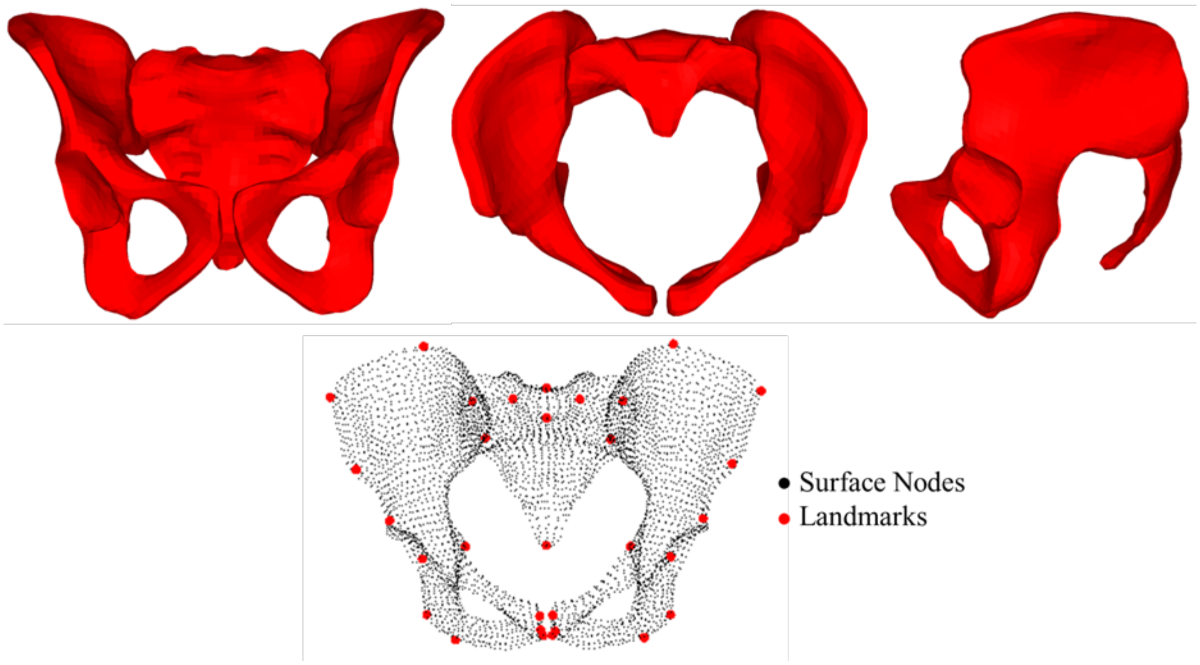

Figure 1a. Small female pelvis geometry predicted by a statistical pelvis geometry model.

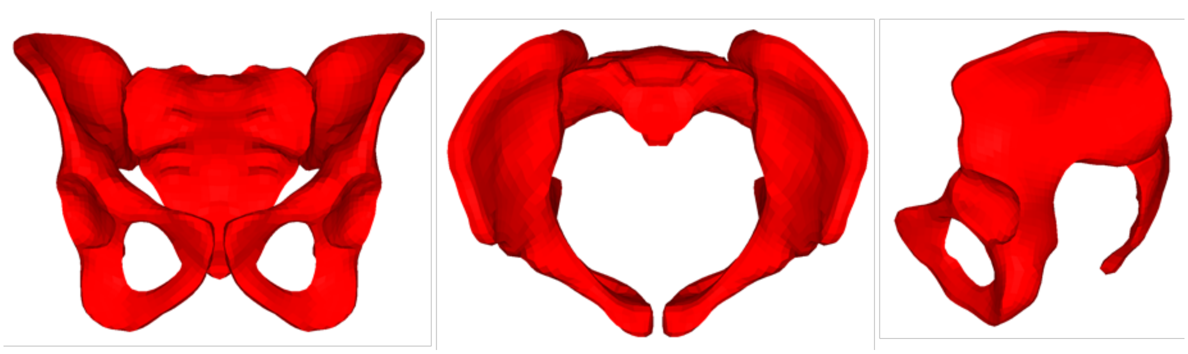

Figure 1b. Small female pelvis geometry made symmetric by reflecting the left side to the right.

3.2 Comparison of Pelvis Models

The Euclidean distance between select landmarks for the symmetric SFPM, the small female from the AMVO study (Schneider et al. 1983), the small female Hybrid III, and the scaled midsize male model are given in Table 1. Most of the dimensions between the SFPM and the AMVO study are similar, except for the right and left hip joint center to ischial tuberosity, which is about 10 percent larger in the SFPM. Several of the distances are not similar, notably the bispinous breadth, between the SFPM and the Hybrid III since the small female Hybrid III dimensions were obtained from Reynolds et al. (1981), and this study was used to develop the small female ATD pelvis.

Table 1. Comparison of small female pelvis model, AMVO, small female Hybrid III, and scaled midsize male model dimensions

Landmark-to-Landmark Distance	Small Female Pelvis Model (mm)	Small Female AMVO (mm)	Small Female Hybrid III*** (mm)	Scaled Midsize Male Model (mm)
Left Hip Joint Center to Right Hip Joint Center	160	160	160	140
Left ASIS* to Right ASIS* (Bispinous Breadth)	204	206	218	206
Left Hip Joint Center to Left ASIS*	82	80	82	75
Right Hip Joint Center to Right ASIS*	82	80	82	76
Left Hip Joint Center to Left Ischial Tuberosity	75	69	74	79
Right Hip Joint Center to Right Ischial Tuberosity	75	69	74	78
Right Iliocristale to Left Iliocristale (Iliac Breadth)	168	N/A	178	153
Left PSIS** to Right PSIS**	105	N/A	86	77
Left ASIS* to Left PSIS**	142	N/A	131	139
Right ASIS* to Right PSIS**	142	N/A	131	141
Left Iliocristale to Left Ischial Tuberosity	191	N/A	185	190
Right Iliocristale to Right Ischial Tuberosity	191	N/A	185	189

*Anterior superior iliac spine

** Posterior superior iliac spine

*** This data comes from Reynolds et al. (1981), which was used to develop the small female Hybrid III pelvis.

Figure 2 shows a comparison between the symmetric SFPM and the Hybrid III small female pelvis, aligned using a least-squares alignment based on the hip joint centers, anterior superior iliac spine (ASIS) landmarks, and the most inferior landmarks on the ischial tuberosities. Differences exist in many parts of the geometry, such as the bispinous breadth (left to right ASIS) and locations of the ischial tuberosities. The shapes of the pubic rami, anterior superior pelvis, iliac wings, ischial tuberosities, and sacrum also differ between the SFPM and the small female Hybrid III pelvis.

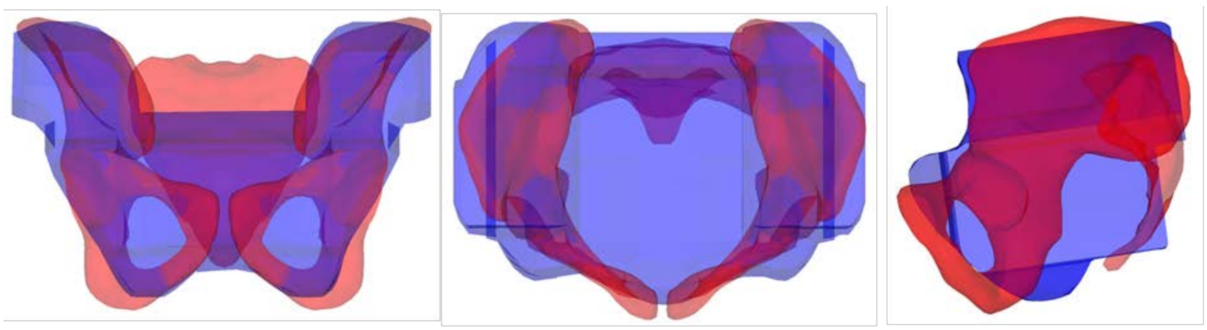

Red: Small Female Pelvis Model
Blue: Hybrid III Small Female Pelvis

Figure 2. Comparison of SFPM geometry and Hybrid III geometry.

When the pelvises were aligned to the ischial tuberosities as shown in Figure 3a, similar to how the pelvis would sit in a vehicle seat, the small female pelvis model average ASIS point was 2 mm higher than the Hybrid III ASIS point. When the pelvises were aligned to the hip joint centers as shown in Figure 3b, the small female pelvis model average ASIS point was 9 mm lower than the Hybrid III.

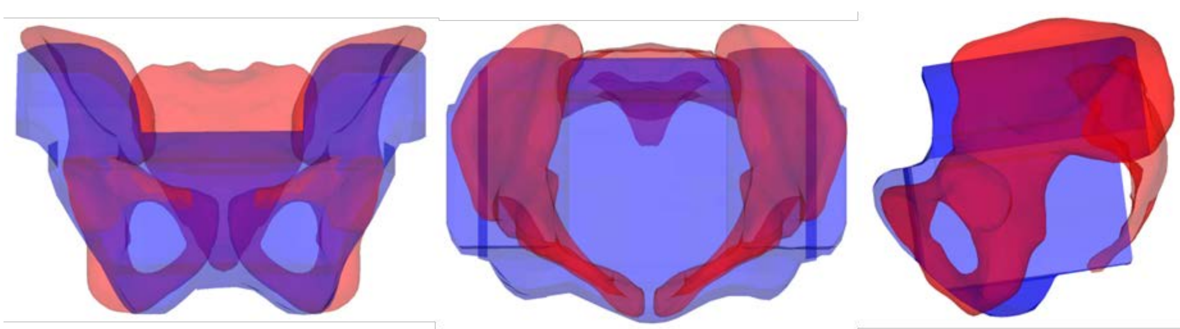

Red: Small Female Pelvis Model
Blue: Hybrid III Small Female Pelvis

Figure 3a. Comparison of SFPM geometry and Hybrid III geometry aligned to ischial tuberosities.

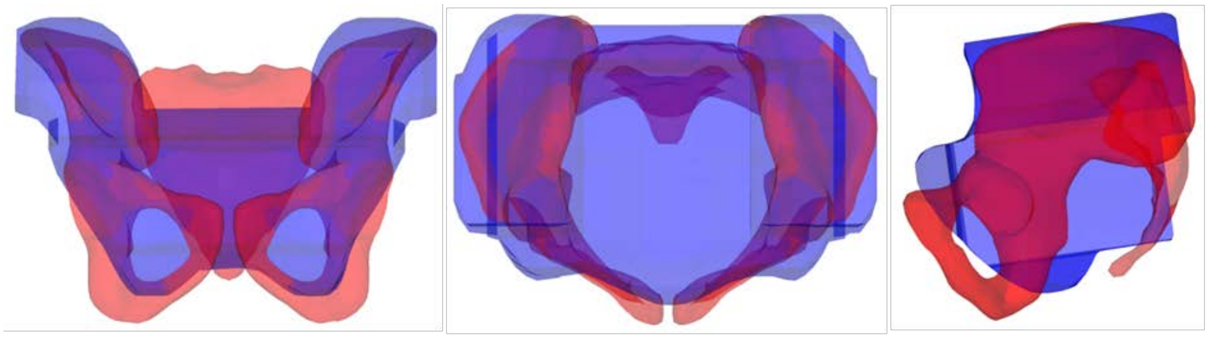

Red: Small Female Pelvis Model
Blue: Hybrid III Small Female Pelvis

Figure 3b. Comparison of SFPM geometry and Hybrid III geometry aligned to hip joint centers.

Figure 4 shows the comparison between the small female pelvis model and the midsize male scaled to the small female bispinous breadth. Again, differences can be seen in the overall dimensions and shape, such as the anterior to posterior depth and ischium breadth, as well as the shape of the pubic rami and ischial tuberosities. The male and female surfaces were aligned about the centroid of the nodal coordinates.

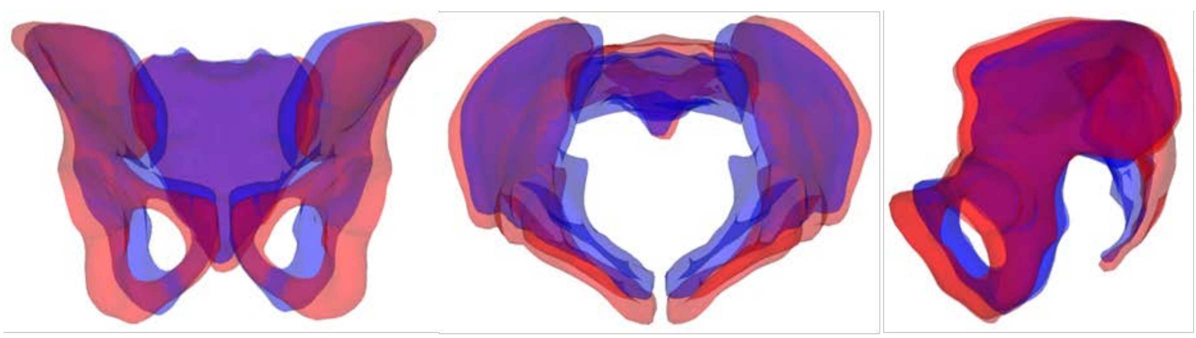

Red: Small Female Pelvis Model
Blue: Scaled Male Pelvis

Figure 4. Comparison of SFPM geometry and scaled male geometry.

4 Discussion and Conclusions

Target surface geometry for the small female pelvis was predicted using a statistical model of pelvis geometry developed from medical imaging data. The resulting surface was compared to the Hybrid III small female pelvis and to a surface generated by applying uniform scaling to the midsize male pelvis. The small female pelvis model was taller than both the Hybrid III pelvis and scaled male pelvis. Aligning the small female pelvis model and the Hybrid III pelvis model in what is believed to be the most realistic way possible (aligning the models at the ischial tuberosities) resulted in a 2 mm difference in ASIS height along with differences in the shape of the pelvis around the ASIS, which could alter the interaction between the pelvis and lap belt. The small female pelvis model also had different shapes for the pubic rami, ischial tuberosities, and sacrum than the Hybrid III small female pelvis, such as greater separation between the ischial tuberosities and a different location of the ischial tuberosities, which may affect interactions with vehicle seats. Finally, the SFPM developed in this study represents a geometry that is appropriate for the small female 5th percentile target and, as a result, improves upon the work done by Reynolds et al. (1981), who developed a small female target by averaging geometries of pelvises from women under the 25th percentile in stature.

Appendix A – Small Female Pelvis Landmark Coordinates

Table A. List of landmark coordinates for the small female pelvis model

Landmark	x (mm)	y (mm)	z (mm)
Superior iliac wing_L	-91.1	84.1	54.6
Superior iliac wing_R	-91.1	-84.1	54.6
Lateral iliac wing_L	-43.1	123.0	31.1
Lateral iliac wing_R	-43.1	-123.0	31.1
Posterior superior iliac spine_L	-132.1	52.3	15.7
Posterior superior iliac spine_R	-132.1	-52.3	15.7
Anterior superior iliac spine_L	0.0	101.9	0.0
Anterior superior iliac spine_R	0.0	-101.9	0.0
Posterior inferior iliac spine_L	-127.4	44.7	-11.2
Posterior inferior iliac spine_R	-127.4	-44.7	-11.2
Anterior inferior iliac spine_L	-14.5	88.5	-39.3
Anterior inferior iliac spine_R	-14.5	-88.5	-39.3
Superior first sacral segment_Anterior	-64.7	0.0	11.2
Superior first sacral segment_Posterior	-88.0	0.0	28.2
Superior first sacral segment_L	-77.2	21.2	22.6
Superior first sacral segment_R	-77.2	-21.2	22.6
Anterior superior symphyseal pole_L	5.7	5.8	-92.4
Anterior superior symphyseal pole_R	5.7	-5.8	-92.4
Anterior symphyseal pole_L	-0.7	3.4	-104.1
Anterior symphyseal pole_R	-0.7	-3.4	-104.1
Inferior symphyseal pole_L	-21.3	5.1	-110.4
Inferior symphyseal pole_R	-21.3	-5.1	-110.4
Lateral ischial tuberosity_L	-67.5	80.8	-121.2
Lateral ischial tuberosity_R	-67.5	-80.8	-121.2
Inferior ischial tuberosity_L	-70.8	64.5	-134.6
Inferior ischial tuberosity_R	-70.8	-64.5	-134.6
Inferior last sacral segment	-122.3	0.0	-87.7
Anterior acetabulum edge_L	-19.6	71.2	-66.9
Anterior acetabulum edge_R	-19.6	-71.2	-66.9
Ischial spine_L	-89.0	56.7	-77.0
Ischial spine_R	-89.0	-56.7	-77.0
Hip joint center_L	-44.3	80.2	-66.3
Hip joint center_R	-44.3	-80.2	-66.3

The landmarks are given in the set of axes defined by Reynolds et al. (1981). Figure A shown below demonstrates how the axes are defined with the y-axis determined by the line between the ASIS points and the z-axis perpendicular to the y-axis through the midpoint of the pubic symphysis.

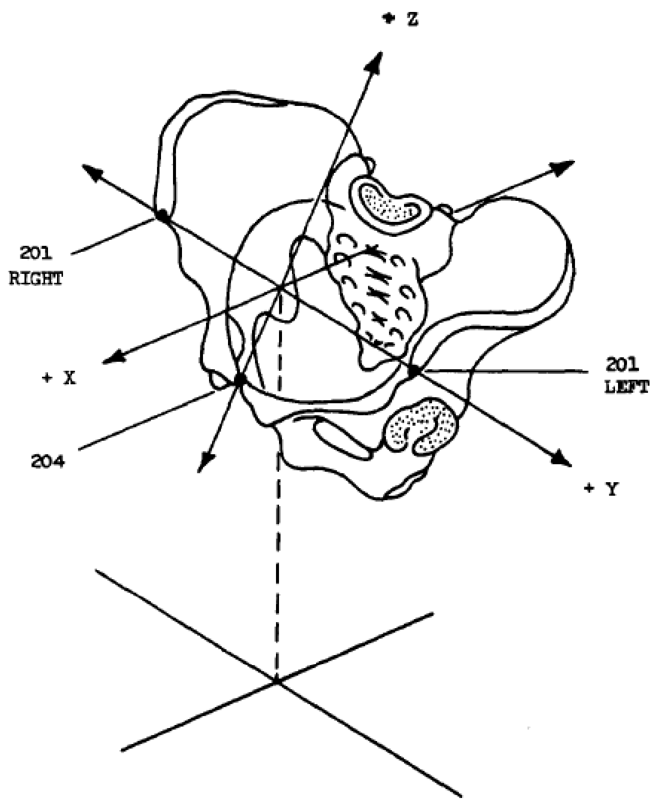

Figure A. The Reynolds et al. (1981) pelvis axis system.

Acknowledgements

This project was funded by the National Highway Traffic Safety Administration under contract number DTNH22-10-H-00288 and the National Science Foundation under award number 1300815. The authors would like to thank Kyle Boyle for his assistance with generating the Hybrid III pelvis surface and the University of Michigan students who extracted pelvis geometry.

References

Besnault, B., Lavaste, F., Guillemot, H., Robin , S., and Le Coz, J. Y., 1998. A parametric finite element model of the human pelvis. Stapp Car Crash Conference 42, 33-46.

Carter, P. M., Flannagan, C. A. C., Reed, M. P., Cunningham, R. M., and Rupp, J. D., 2014. Comparing the effects of age, BMI and gender on severe injury (AIS 3+) in motor-vehicle crashes. Accident Analysis and Prevention 72, 146-160.

Humanetics Innovative Solutions, Plymouth, MI. Hybrid III Crash Test Dummies.

Klein, K. F., 2015. Use of parametric finite element models to investigate effects of occupant characteristics on lower-extremity injuries in frontal crashes. University of Michigan.

Klinich, K. D., Reed, M. P, Manary, M. A., and Orton, N. R., 2010. Development and testing of a more realistic pelvis for the Hybrid III 6YO ATD. Traffic Injury Prevention, 11, 606-612.

Reed, M. P., Sochor, M. M., Rupp, J. D., Klinich, K. D., and Manary, M. A., 2009. Anthropometric specification of child crash dummy pelves through statistical analysis of skeletal geometry. Journal of Biomechanics, 42, 1143-1145.

Reynolds, H. M., Clyde, C. C., and Young, J. W., 1981. Spatial geometry of the human pelvis. Federal Aviation Administration, Memorandum Report No. AAC-119-81-5.

Rhule, D. A. and Backaitis, S., 1998. Development and evaluation of the hybrid III fifth percentile female crash test dummy. NHTSA Docket No. 1998-4283-6.

Riggs, B. L., Melton III, L. J., Robb, R. A., Camp, J. J., Atkinson, E. J., Peterson, J. M., Rouleau, P. A., McCollough, C. H., Bouxsein, M. L. and Khosla, S., 2004. Population-based study of age and sex differences in bone volumetric density, size, geometry, and structure at different skeletal sites. Journal of Bone and Mineral Research 19, 1945-1954.

Rupp, J. D. and Flannagan, C.A.C., 2011. Effects of occupant age on AIS 3+ injury outcome determined from analyses of fused NASS/CIREN data. Proceedings of the Informal Group for the Harmonization of WorldSID Dummies, Belgium.

Schneider, L. W., Robbins, D. H., Pflüg, M. A., and Snyder, R. G., 1983. Development of anthropometrically based design specifications for an advanced adult anthropomorphic dummy family, volume 1. UMTRI-83-53-1.

Wang, S.C., Brede, C., Lange, D., Poster, G.S., Lange, A.W., Kohoyda-Inglis, C., Sochor, M.M., Ipaktchi, K. and Rowe, S.A., 2004. Gender differences in hip anatomy: possible implications for injury tolerance in frontal collisions. Proc. Association for the Advancement of Automotive Medicine 48, 287-301.